On the motion of various vertical modes of transient, very long waves[1]

II. *The Spherical Case*

By A. WIIN-NIELSEN, *Department of Meteorology and Oceanography, The University of Michigan, Ann Arbor, Mich., USA*

(Manuscript received November 2, 1970)

ABSTRACT

The problem of motion of atmospheric waves superimposed on a basic state of no motion and a constant temperature lapse rate has been solved. It is found that there exists several vertical modes. For each of the vertical modes there exists several horizontal modes, each moving with a separate speed and having a certain south–north variation of the amplitudes of the geopotential, the stream function and the velocity potential.

The solution is obtained by expanding each variable for each vertical mode in a truncated series of associated Legendre functions. It is found that the waves connected with the first vertical mode behave as waves in a homogeneous fluid with a free surface, while the waves connected with the second and third vertical modes move with a much smaller speed. All waves move from east to west. The structure of the waves is compared with the structure as obtained from atmospheric observations with fair agreement.

The solutions are compared with the motion of transient, very long waves as obtained from a quasi-geostrophic model.

1. Introduction

In a recent paper (Wiin-Nielsen, 1970, hereafter referred to as I) an analysis was made of the motion and structure of transient, very long waves in the atmosphere. The investigation was based on a perturbation analysis of the waves superimposed on a basic state characterized by no motion and a constant temperature lapse rate. The main results of the investigation described in I were that there exists an infinite number of vertical modes, each characterized by an equivalent depth and each with a separate speed of propagation, that the basic mode depends critically on the lower boundary condition and can be described as the divergent barotrophic mode, because it corresponds to the mode present in a homogeneous fluid with a free surface, and that the higher vertical modes are described with good approximation by Burger's (1958) equations and by a simplified lower boundary condition ($\omega = dp/dt = 0$ at $p = p_0 = 100$ cb).

In order to keep the analysis relatively simple, a beta-plane geometry was adopted in I. The advantage of this approach is that it is possible to obtain a formula for the phase speed in a closed form, and it becomes rather straightforward to analyze the influence of the various parameters which enter into the problem. These parameters are the equivalent depth, the width of the channel, the horizontal wavelength, and the values of the Coriolis parameter (f) and the Rossby parameter ($\beta = df/dy$). However, it has been shown that the beta-plane approximation cannot be justified as a satisfactory approximation when we are dealing with the largest horizontal scale (Phillips, 1963). If we want to make a more detailed comparison with the observed motion in the atmosphere than was possible in I, it becomes necessary to replace the beta-plane geometry by the more realistic spherical geometry. The main purpose of this paper is to report the results

[1] Publication No. 188 from the Department of Meteorology and Oceanography, The University of Michigan. Research supported by the National Science Foundation under Grant GA-16166.

of such an investigation. The investigation will follow the same lines as in I, the only difference being the adoption of spherical geometry.

2. The model

The perturbation equations using the same basic state as in I are

$$\frac{\partial u}{\partial t} = -\frac{1}{a\cos\varphi}\frac{\partial\phi}{\partial\lambda} + fv$$

$$\frac{\partial v}{\partial t} = -\frac{1}{a}\frac{\partial\phi}{\partial\varphi} - fu$$

$$\nabla\cdot\mathbf{v} + \frac{\partial\omega}{\partial p} = 0$$

$$\frac{\partial}{\partial t}\left(\frac{\partial\phi}{\partial p}\right) + \bar{\sigma}\omega = 0 \qquad (2.1)$$

where the notations are the same as in I except that λ is longitude, φ latitude, and a the radius of the earth. It becomes convenient to replace the first two equations in (2.1) by the corresponding vorticity and divergence equations obtained in the usual manner. They are

$$\frac{\partial\zeta}{\partial t} = -f\nabla\cdot\mathbf{v} - \frac{2\Omega}{a}\cos\varphi v$$

$$\frac{\partial\nabla\cdot\mathbf{v}}{\partial t} = -\nabla^2\phi + f\zeta - \frac{2\Omega}{a}\cos\varphi u \qquad (2.2)$$

where the vorticity ζ is:

$$\zeta = \frac{1}{a\cos\varphi}\left(\frac{\partial v}{\partial\lambda} - \frac{\partial u\cos\varphi}{\partial\varphi}\right) \qquad (2.3)$$

and the divergence $\nabla\cdot\mathbf{v}$ is:

$$\nabla\cdot v = \frac{1}{a\cos\varphi}\left(\frac{\partial u}{\partial\lambda} + \frac{\partial v\cos\varphi}{\partial\varphi}\right) \qquad (2.4)$$

while ∇^2 denotes the spherical Laplacian

$$\nabla^2 = \frac{1}{a^2}\nabla_s^2 = \frac{1}{a^2} \times \left[\frac{1}{\cos^2\varphi}\frac{\partial^2}{\partial\lambda^2} + \frac{1}{\cos\varphi}\frac{\partial}{\partial\varphi}\left(\cos\varphi\frac{\partial}{\partial\varphi}\right)\right] \qquad (2.5)$$

where ∇_s^2 is a notation for the quantity in the bracket in (2.5).

The horizontal flow will be described by a stream function ψ and a velocity potential χ. In terms of these functions we have:

$$u = -\frac{1}{a}\frac{\partial\psi}{\partial\varphi} + \frac{1}{a\cos\varphi}\frac{\partial\chi}{\partial\lambda}$$

$$v = \frac{1}{a\cos\varphi}\frac{\partial\psi}{\partial\lambda} + \frac{1}{a}\frac{\partial\chi}{\partial\varphi} \qquad (2.6)$$

while $\zeta = \nabla^2\psi$ and $\nabla\cdot\mathbf{v} = \nabla^2\chi$.

As will be seen later our problem will be analogous to the problem treated by Eliasen & Machenhauer (1969) using a homogeneous fluid with a free surface. To ease a comparison with this study we shall adopt the same notations and scaling whenever possible. In agreement with this statement we write the perturbations of the stream function, the velocity potential, the geopotential and the vertical velocity in the form:

$$\psi = \psi_m(\varphi, p)\,e^{im(\lambda - ct)}$$

$$\chi = i\chi_m(\varphi, p)\,e^{im(\lambda - ct)}$$

$$\phi = 2\Omega\,\eta_m(\varphi, p)\,e^{im(\lambda - ct)}$$

$$\omega = \frac{i}{a^2}\omega_m(\varphi, p)\,e^{im(\lambda - ct)} \qquad (2.7)$$

It is furthermore convenient to introduce the nondimensional phase speed

$$s = \frac{\nu}{2\Omega} = -\frac{mc}{2\Omega} \qquad (2.8)$$

where ν is the frequency.

When (2.7) is substituted in (2.2) and the last two equations in (2. 1), and we furthermore introduce the new coordinate $\mu = \sin\varphi$, we obtain the following system of equations:

$$s\nabla_s^2\psi_m + m\psi_m + (1-\mu^2)\frac{\partial\chi_m}{\partial\mu} + \mu\nabla_s^2\chi_m = 0$$

$$s\nabla^2\chi_m + m\chi_m + (1-\mu^2)\frac{\partial\psi_m}{\partial\mu} + \mu\nabla_s^2\psi_m = \nabla^2\eta_m \qquad (2.9)$$

$$\nabla_s^2\chi_m + \frac{\partial\omega_m}{\partial p} = 0$$

$$s\frac{\partial \eta_m}{\partial p} + \frac{\bar{\sigma}}{4\Omega^2 a^2}\omega_m = 0$$

where ∇_s^2 in terms of the new coordinate μ is:

$$\nabla_s^2 = \frac{\partial}{\partial \mu}\left[(1-\mu^2)\frac{\partial}{\partial \mu}\right] - \frac{m^2}{1-\mu^2} \qquad (2.10)$$

It is a straightforward matter to eliminate ω_m between the last two equations in (2.9). These two equations are then replaced by the equation:

$$\nabla_s^2 \chi_m - s4\Omega^2 a^2 \frac{\partial}{\partial p}\left(\frac{1}{\bar{\sigma}}\frac{\partial \eta_m}{\partial p}\right) = 0 \qquad (2.11)$$

An inspection of the first two equations in (2.9) and equation (2.11) reveals that these equations can be solved by a separation of variables in the form:

$$\psi_m(\mu, p) = F(p)\hat{\psi}_m(\mu)$$

$$\chi_m(\mu, p) = F(p)\hat{\chi}_m(\mu)$$

$$\eta_m(\mu, p) = F(p)\hat{\eta}_m(\mu) \qquad (2.12)$$

if $F(p)$ satisfies the equation:

$$\frac{d}{dp}\left(\frac{1}{\bar{\sigma}}\frac{dF}{dp}\right) + \frac{1}{gh}F = 0 \qquad (2.13)$$

where $-(gh)^{-1}$ is the constant of separation. We note that (2.13) is identical with the vertical structure equation found in I. The solutions to (2.13), including the discussion of the various boundary conditions, can therefore be adopted without change from I. We have therefore from the previous investigation all the numerical values of the equivalent depths listed in Tables 1–4 of I.

Introducing (2.12) and (2.13) in the first two equations of (2.9) and equation (2.11) we get the following equations for $\hat{\psi}_m$, $\hat{\chi}_m$, and $\hat{\eta}_m$:

$$s\nabla_s^2 \hat{\psi}_m + m\hat{\psi}_m + (1-\mu^2)\frac{\partial \hat{\chi}_m}{\partial \mu} + \mu\nabla_s^2 \hat{\chi}_m = 0$$

$$s\nabla_s^2 \hat{\chi}_m + \hat{\chi}_m + (1-\mu^2)\frac{\partial \hat{\psi}_m}{\partial \mu} + \mu\nabla_s^2 \hat{\psi}_m = \nabla_s^2 \hat{\eta}_m$$

$$Q\nabla_s^2 \hat{\chi}_m + s\hat{\eta}_m = 0 \qquad (2.14)$$

where $$Q = \frac{gh}{4\Omega^2 a^2}$$

The system (2.14) is completely analogous to the system solved by Eliasen & Machenhauer (1969) for their case of a homogeneous fluid with a free surface. In that case h is simply the depth of the fluid which they took to be 8 800 m resulting in a value of $Q = 0.1$. In the present case we have removed the arbitrary choice of the equivalent depth which is determined by the solution of (2.13) as described in I. These values of h determine our values of Q in the system (2.14).

Since the system (2.14) is completely equivalent to the system of equations presented by Eliasen & Machenhauer (1969) we shall adopt their method of solution which consists of expanding each of the variables $\hat{\psi}_m$, $\hat{\chi}_m$, and $\hat{\eta}_m$ in a series of associated Legendre functions. The reader is referred to the paper by Eliasen & Machenhauer (1969) for the details of this procedure. It suffices to mention that each series is truncated at a certain place which determines the degree of accuracy with which the eigenvalues are determined. While the convergence of the series is rapid for values of Q equal to 0.1, it turns out that the smaller values of Q which correspond to the higher vertical modes require more terms in the series in order to give good accuracy in the determination of the eigenvalues. The numerical results of the study will be presented in the next section including a discussion of the meridional structure of the waves.

3. Numerical results

The series of associated Legendre functions used in order to obtain appropriate solutions to the system (2.14) are of the form

$$\hat{a}_m(\mu) = \sum_{r=0}^{R} A(m, m+2r)\, P(m, m+2r, \mu) \qquad (3.1)$$

where $\hat{a}_m$ can be either $\hat{\psi}_m$, $\hat{\chi}_m$, or $\hat{\eta}_m$, if $\hat{a}_m(\mu)$ is an even function of μ, i.e., $\hat{a}_m(\mu)$ is symmetric around the equator. On the other hand, if $\hat{a}_m(\mu)$ is an odd function, i.e., antisymmetric around the equator, we use a series of the form

$$\hat{a}_m(\mu) = \sum_{r=0}^{R} A(m, m+2r+1)\, P(m, m+2r+1, \mu) \qquad (3.2)$$

Table 1. *Successive approximations to the eigenvalues corresponding to Rossby waves* ($m = 1$, $Q = 0.1$)

$\hat{\eta}_m$	$R=0$	$R=1$	$R=2$	$R=3$	$R=4$	$R=5$	$R=6$
odd	−278.69	−297.81	−298.03	−298.03	−298.03	−298.03	−298.03
even	−73.92	−68.52	−68.34	−68.34	−68.34	−68.34	−68.34
odd		−41.14	−41.76	−41.77	−41.77	−41.77	−41.77
even		−29.99	−28.48	−28.46	−28.46	−28.46	−28.46
odd			−20.31	−20.43	−20.43	−20.43	−20.43
even			−15.79	−15.26	−15.26	−15.26	−15.26
odd				−11.74	−11.77	−11.77	−11.77
even				−9.56	−9.34	−9.34	−9.34
odd					−7.56	−7.57	−7.57
even					−6.36	−6.26	−6.26
odd						−5.25	−5.25
even						−4.53	−4.47
odd							−3.85
even							−3.38

In (3.1) and (3.2) $P(m, n, \mu)$ is the associated Legendre function, while $A(m, n)$ is the unknown coefficient. It is seen from (2.14) that if $\hat{\eta}_m$ and $\hat{\chi}_m$ are even functions of μ, then $\hat{\psi}_m$ is odd and vice versa. R determines the point at which the series (3.1) and (3.2) are truncated. The minimum value of R is clearly $R = 0$. We would expect on the other hand that a larger value of R would give a more accurate determination of the eigenvalues.

The basic equations (2.1) of the problem indicate that we can expect to find eigenvalues corresponding to gravity-inertial waves and other eigenvalues corresponding to Rossby-type waves. This was also clearly indicated by the solutions presented by Eliasen & Machenhauer (1969) for $Q = 0.1$. In this study we shall only be interested in the Rossby-type waves although all eigenvalues were determined by the numerical solutions of (2.14). The eigenvalues corresponding to gravity-inertial waves are easily recognized from the numerical solution because they appear in pairs and have large numerical values.

A fundamental problem in this procedure is the numerical value of R necessary to insure an accurate determination of the eigenvalues. It is seen from (2.14), (3.1), (3.2), and the equations presented by Eliasen & Machenhauer (1969) that $R = 0$ leads to a cubic equation for the eigenvalue. Two of the roots in this equation correspond to waves of the gravity type,

Table 2. *Successive approximations to the eigenvalues corresponding to Rossby waves* ($m = 1$, $Q = 0.0039$)

$\hat{\eta}_m$	$R=0$	$R=1$	$R=2$	$R=3$	$R=4$	$R=5$	$R=6$
odd	−60.57	−116.96	−147.60	−157.54	−159.17	−159.34	−159.35
even	−11.08	−15.80	−16.07	−15.32	−14.99	−14.93	−14.93
odd		−4.65	−6.88	−8.41	−9.03	−9.18	−9.19
even		−4.39	−6.22	−7.08	−6.97	−6.77	−6.72
odd			−3.37	−4.26	−4.92	−5.24	−5.33
even			−3.31	−4.12	−4.59	−4.60	−4.49
odd				−2.87	−3.39	−3.67	−3.82
even				−2.84	−3.27	−3.52	−3.50
odd					−2.54	−2.84	−3.02
even					−2.52	−2.80	−2.91
odd						−2.24	−2.47
even						−2.22	−2.43
odd							−1.97
even							−1.95

Table 3. *Successive approximations to the eigenvalues corresponding to Rossby waves* ($m = 1$, $Q = 0.0018$)

$\hat{\eta}_m$	$R = 0$	$R = 1$	$R = 2$	$R = 3$	$R = 4$	$R = 5$	$R = 6$
odd	−35.92	−79.86	−110.14	−126.79	−132.66	−133.96	−134.15
even	− 5.72	− 9.70	− 11.02	− 10.85	− 10.43	− 10.22	− 10.17
odd		− 2.24	− 3.55	− 4.79	− 5.64	− 6.04	− 6.17
even		− 2.12	− 3.27	− 4.26	− 4.73	− 4.71	− 4.57
odd			− 1.69	− 2.19	− 2.73	− 3.16	− 3.14
even			− 1.62	− 2.13	− 2.63	− 2.97	− 3.06
odd				− 1.44	− 1.73	− 2.03	− 2.28
even				− 1.43	− 1.71	− 1.99	− 2.20
odd					− 1.32	− 1.51	− 1.69
even					− 1.32	− 1.50	− 1.76
odd						− 1.23	− 1.37
even						− 1.23	− 1.36
odd							− 1.15
even							− 1.14

while the third root is the first approximation to the speed of one of the possible Rossby waves. The next approximation will be $R = 1$ which gives an eigenvalue problem corresponding to a sixth degree equation. Among the six roots of this equation two will correspond to Rossby-type waves. In general, we get $(R+1)$ Rossby-type wave speeds if the series (3.1) and (3.2) are truncated at a certain value R. We shall later be concerned with the interpretation of the various numerical values by investigating the meridional structure of the waves. However, at the moment we are mainly concerned with the accuracy of the solution for given values of R and Q. As examples we present the values given in Tables 1–3.

Table 1 gives the eigenvalues corresponding to Rossby waves expressed as the wave speed using the unit, deg. long. day^{-1}, for the case of wave number 1 (i.e., $m = 1$) and $Q = 0.1$. For each value of R we present all the eigenvalues corresponding to both the odd and the even case. The first column gives the symmetry of the height field. From this it is known that the velocity potential will have the same symmetry while the stream function will be of the opposite kind. Furthermore, we have ordered the eigenvalues according to their absolute value. It is seen that if we are interested in only the numerically largest eigenvalues it would in this case be sufficient to select a rather small value of R as was done by Eliasen & Machenhauer (1969).

Table 2 provides similar information for the case $m = 1$, $Q = 0.0039$ corresponding to the second vertical mode as described in I if the lapse rate is 8.5°K km^{-1}. It is seen from this table that larger values of R are necessary to provide sufficient accuracy. However, $R = 6$ is sufficient to obtain the necessary accuracy, in particular, for the numerically largest values of the wave speed.

Table 3 is similar to Tables 1 and 2 except that this table gives the various approximations to the eigenvalues for $Q = 0.0018$ corresponding to the third vertical mode for the same lapse rate. It is seen that the convergence becomes slower as the value of Q decreases. However, good accuracy is obtained for $R = 6$ for the numerically large values, and the remaining values are numerically small.

Based upon the information in Tables 1–3 and similar tables for other values of m and Q (not reproduced) it was decided to use $R = 6$ for all calculations. All values of the wave speed, expressed in deg. long. day^{-1}, for $m = 1$, 2, and 3 and the values of Q corresponding to the first three vertical modes (lapse rate: 8.5°K km^{-1}) are given in Table 4. The values for $Q = 0.1$ are naturally only an extension of the wave speeds already considered by Eliasen & Machenhauer (1969). We shall be interested in the computed wave speeds for the second and third vertical modes corresponding to the values $Q = 0.0039$ and $Q = 0.0018$. With exception of the values in the first row in Table 4 we find relatively small numerical values of the wave speed for these two vertical modes.

Table 4. *Values of the phase speed for Rossby-type waves in the unit: deg. long. day*$^{-1}$ ($R = 6$)

Height		$Q = 0.1$			$Q = 0.0039$			$Q = 0.0018$		
		$m = 1$	$m = 2$	$m = 3$	$m = 1$	$m = 2$	$m = 3$	$m = 1$	$m = 2$	$m = 3$
odd	c_1	−298.0	−110.0	−57.3	−159.3	−70.1	−41.3	−134.2	−60.4	−36.4
even	c_1	−68.3	−46.9	−31.8	−14.9	−14.1	−12.8	−10.2	−9.8	−9.2
odd	c_2	−41.8	−29.7	−21.4	−9.2	−8.8	−8.2	−6.2	−6.0	−5.8
even	c_2	−28.5	−20.8	−15.6	−6.7	−6.5	−6.1	−4.6	−4.4	−4.3
odd	c_3	−20.4	−15.4	−11.9	−5.3	−5.2	−4.9	−3.4	−3.4	−3.3
even	c_3	−15.2	−11.8	−9.4	−4.5	−4.3	−4.1	−3.1	−3.0	−2.9

This result is in very good agreement with the results obtained in I. When we furthermore recall that the values appearing in Table 4 are computed under the assumption of no motion in the basic state, we observe that all the waves will move with a speed smaller than the basic current.

The only investigation which has been made up to the present time of the wave speeds of the second and higher vertical modes is by Bradley & Wiin-Nielsen (1968). The major emphasis in this study was on the vertical and horizontal structure of the waves, and the wave speeds were obtained by a simple visual inspection of the variation of the phase angle as a function of time. There is clearly a need for an empirical investigation of the motion of the waves in the horizontal fields related to the higher vertical modes using a procedure similar to the one employed by Eliasen & Machenhauer (1969) based on quadrature spectra. However, there is at least qualitative agreement between the results given in Table 4 and those presented by Bradley & Wiin-Nielsen (1968) because most wave speeds are numerically small, implying that they will move eastward relative to the earth when corrections have been made for a basic zonal current different from zero. It is furthermore in agreement with the observational study that the wave speeds for the second and third vertical modes vary rather slowly with the longitudinal wave number in contrast to the first vertical mode which varies very markedly with m, the longitudinal wave number. Finally, the order of magnitude of the computed wave speeds when corrected for the basic current compares favorably with those obtained from the observational study.

The major weakness of a study of transient waves in a system as simple as the basic state employed in this study is naturally that one obtains infinitely many wave speeds. The values listed in Table 4 are the wave speeds obtained for the value $R = 6$, but if we increase R we would naturally obtain additional values. On the basis of the present analysis it is impossible to determine if all the possible waves are present in the atmosphere, or if only certain waves, excited by instability mechanisms or heat sources, will dominate the atmospheric flow. In an investigation to be published later it will be demonstrated that some transient, ultra-long waves are unstable when the basic state has vertical wind shear. This investigation is based upon Burger's assumption and a simplified lower boundary condition as discussed in I.

From an empirical point of view we have considerable evidence that only certain modes of atmospheric motion are present with considerable amounts of energy in the atmosphere. The major evidence concerning the vertical and meridional structure is given by Bradley & Wiin-Nielsen (1968) in terms of empirical ortho-

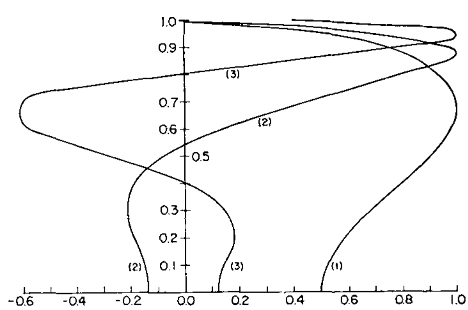

Fig. 1. Normalized height field as a function of $\mu = \sin \varphi$ for the first vertical mode and for the first three Rossby waves. Symmetric case.

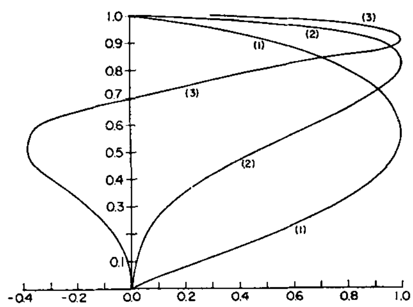

Fig. 2. As Fig. 1. Antisymmetric case.

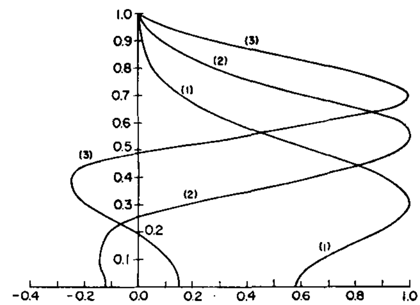

Fig. 3. Normalized height field as a function of $\mu = \sin\varphi$ for the second vertical mode and for the first three Rossby waves. Symmetric case.

gonal functions and by Eliasen & Machenhauer (1969) in terms of associated Legendre functions. These empirical results can now be compared with the theoretical results obtained here and in I. With respect to the vertical structure functions a comparison was already made in I. We shall here be concerned with the meridional structure of the waves whose wave speed was given in Table 4.

For a given value of the wave speed we can go back to the linear equations which came from substituting the series (3.1) and (3.2) in (2.14). Setting an arbitrary coefficient in the series of associated Legendre functions equal to unity we may find all the other coefficients in the series for the geopotential, the stream function and the velocity potential. It is then possible to sum the series (3.1) or (3.2) for each of the three variables for any value of μ. We can consequently find $\hat{a}_m(\mu)$ as a function of latitude where $\hat{a}_m(\mu)$ is either the geopotential, the stream function, or the velocity potential. Because there are three parameters (equivalent depth, longitudinal wave number, and the computed phase speed) in each case, it is neither possible nor desirable to display all the latitudinal distributions. It will suffice to give some examples.

Considering the height field it turns out that the normalized functions $\hat{\eta}(\mu)$ are almost the same for the three longitudinal wave numbers $m = 1$, 2, and 3 for the same value of Q and the corresponding values of the phase speed c for the Rossby-type waves. For each value of Q and m we have arranged the phase speeds in a series of numerically decreasing values. Such a series will be denoted c_1, c_2 c_3, ..., as indicated in Table 4.

Fig. 1 shows the normalized distributions $\hat{\eta}_m = \hat{\eta}_m(\mu)$ for the first three values c_1, c_2, and c_3 for the first vertical mode ($Q = 0.1$) and for the symmetric cases, while Fig. 2 gives the analogous distributions for the antisymmetric. cases. Fig. 3 (symmetric cases) and Fig. 4 (antisymmetric cases) show the distributions for the second vertical mode, while Figs. 5 and 6 correspond to the third vertical mode. The curves in Figs. 1–6 are all drawn for $m = 1$ but almost identical curves were obtained for $m = 2$ and $m = 3$ (not reproduced) showing that the meridional distributions are essentially independent of the zonal wave number as also found by Bradley & Wiin-Nielsen (1968) in an observational study.

We notice furthermore that the position of the northernmost maximum in all cases is found further to the north as the index of c increases. The distributions corresponding to $c = c_2$ have one maximum and one minimum in the symmetric cases, but only one maximum in the antisymmetric cases for $0 < \mu < 1$.

The speed and structure of the waves considered in this study are obtained as perturbation solutions using a basic state of no motion

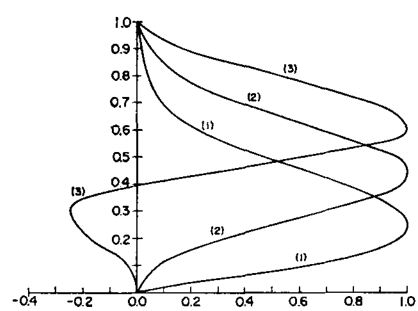

Fig. 4. As Fig. 2. Antisymmetric case.

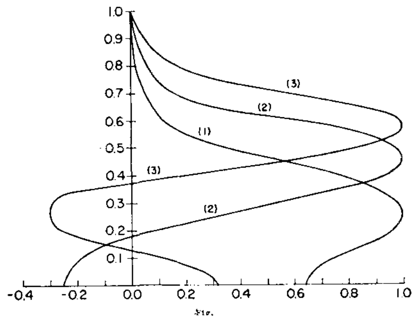

Fig. 5. Normalized height field as a function of $\mu = \sin\varphi$ for the third vertical mode and for the first three Rossby waves. Symmetric case.

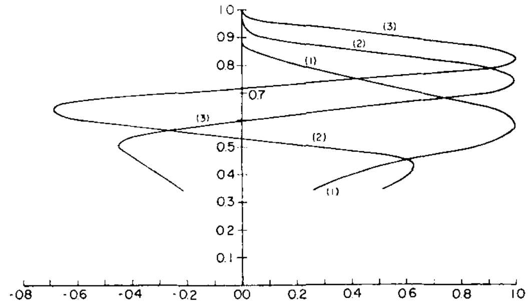

Fig. 7. Normalized height field as a function of $\mu = \sin\varphi$ for the first three Rossby waves based on observations.

and a specified thermal stratification. Since all the waves in this case are neutral, we have no possibility to decide which waves may be observed in the atmosphere. In order to judge whether or not some of the waves appear in atmospheric flow it is therefore necessary to resort to observational studies. It was shown by Bradley (1967) and Bradley & Wiin-Nielsen (1968) using empirical orthogonal functions that it is possible to recognize at least three vertical and four meridional modes. The study, based upon atmospheric data for a three-month period, was unfortunately limited to the latitudinal region north of 20° N. The first three latitudinal modes obtained by Bradley (1967) are given in Fig. 7 as a function of $\mu = \sin\varphi$ and normalized in such a way that the absolute maximum is equal to one. A comparison between Fig. 7 and the theoretical curves in Figs. 1–6 clearly indicates that there is considerable similarity between the two sets of curves. Bradley (1967) found that the meridional distributions in the various horizontal modes were essentially independent of the zonal wave number. This observation was also

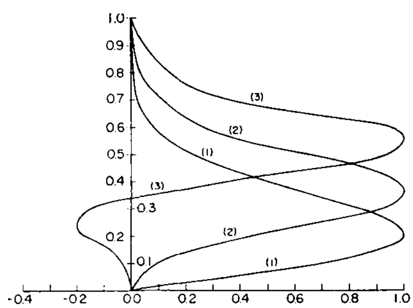

Fig. 6. As Fig. 5. Antisymmetric case.

made in the theoretical study. He found, furthermore, that the horizontal modes were, for practical purposes, independent of the vertical modes. This observation does not hold true for the theoretical modes as can be seen from Figs. 1–6. However, the main difference in the modes is in the low latitudes due to the fact that there are both symmetric and antisymmetric distributions. In the middle and high latitudes there is great similarity between the distributions of $\hat{\eta}_m(\mu)$ for the various vertical modes for the same values of c.

The meridional variation of the functions $\hat{\psi}_m(\mu)$ and $\hat{\chi}_m(\mu)$ was also calculated. However, because no observational study exists with which a comparison can be made, these curves are not reproduced. It is of interest to investigate the vorticity and the divergence of the various modes. These quantities can be obtained from the series expansions for the stream function and the velocity potential. If the expansion of the stream function is

$$\hat{\psi}_m(\mu) = \sum_{r=0}^{R} \Psi(m, m+2r)\, P(m, m+2r, \mu) \qquad (3.3)$$

we find that the vorticity is given by the series

$$\hat{\zeta}_m(\mu) = \sum_{r=0}^{R} (m+2r)(m+2r+1)\, \Psi(m, m+2r) \times P(m, m+2r, \mu) \qquad (3.4)$$

with an analogous expression for the divergence expressed in terms of the coefficients for the velocity potential. It is of special interest to obtain information concerning the ratio of

Table 5. *The ratio of RMS—Values of the divergence and the vorticity*

Height		$Q=0.1$			$Q=0.0039$			$Q=0.0018$		
		$m=1$	$m=2$	$m=3$	$m=1$	$m=2$	$m=3$	$m=1$	$m=2$	$m=3$
even	c_1	0.044	0.027	0.015	0.092	0.130	0.123	0.095	0.150	0.159
	c_2	0.016	0.013	0.010	0.030	0.048	0.055	0.027	0.048	0.059
	c_3	0.004	0.004	0.004	0.020	0.031	0.034	0.018	0.029	0.035
odd	c_1	0.450	0.153	0.063	0.768	0.487	0.319	0.830	0.559	0.388
	c_2	0.047	0.037	0.024	0.074	0.125	0.140	0.065	0.119	0.148
	c_3	0.008	0.008	0.006	0.041	0.063	0.066	0.041	0.068	0.080

the order of magnitude of the divergence to the vorticity in the transient waves, because this ratio indicates whether or not the waves are of a quasi-geostrophic nature. As a measure of the order of magnitude of each of the quantities it was decided to select the root-mean-square values computed for the region from the South Pole to the North Pole $(-1 \leq \mu \leq 1)$. These values were computed from the values of $\hat{\zeta}_m(\mu)$ and $\hat{D}_m(\mu)$, when $D = \nabla^2\chi$ is the divergence.

Table 5 shows the results obtained for the ratio of the RMS values of divergence and vorticity as a function of the vertical mode, the longitudinal wave number, and for the first three Rossby-type waves. The numerical values of c_1, c_2, and c_3 can be obtained from Table 4. We note first of all that the ratio is smaller than unity in all cases. It is secondly seen that the values decrease as the index of c increases. In general, we find that the ratio between divergence and vorticity is smaller than 0.1 for the second and third Rossby-type waves. The exception is in the waves where m is 2 and 3 for the second and third vertical mode, and the height field is antisymmetric. In these four cases we find values between 0.10 and 0.15. For the Rossby waves corresponding to the speeds c_2 and c_3 we can therefore state that the divergence is about one order of magnitude smaller than the vorticity. The same statement cannot be made for the Rossby wave corresponding to c_1 in the case where the height field is antisymmetric, in which case the ratio may be as large as 0.8. These waves have numerically large phase speeds as can be seen from the first row in Table 4, especially in the cases where the ratio is large. It should be stressed that the observational study by Eliasen & Machenhauer (1969) shows that there are no observed waves corresponding to these modes.

4. Quasi-geostrophic modes

It is of interest to investigate to which extent the behavior of the transient very long waves as found and described in the preceding sections can be obtained from a quasi-geostrophic model because such a model is used in some instances for diagnostic and predictive purposes.

The quasi-geostrophic vorticity equation can be written in the form

$$\frac{\partial \nabla^2 \phi}{\partial t} = f_0^2 \frac{\partial \omega}{\partial p} - \frac{2\Omega}{a^2}\frac{\partial \phi}{\partial \lambda} \tag{4.1}$$

where f_0 is a standard value of the Coriolis parameter. In obtaining (4.1) we have already incorporated the same basic state as used earlier in this investigation. Using the same form of the thermodynamic equation as given in the last equation in (2.1) one can eliminate ω between that equation and (4.1) and obtain:

$$\frac{\partial}{\partial t}\left[\nabla^2\phi + \frac{\partial}{\partial p}\left(\frac{f_0^2}{\bar{\sigma}}\frac{\partial \phi}{\partial p}\right)\right] + \frac{2\Omega}{a^2}\frac{\partial \phi}{\partial \lambda} = 0 \tag{4.2}$$

This equation can easily be solved by substituting the perturbation expression for ϕ listed in (2.7) into (4.2), separating the variables according to (2.12), whereby we obtain (2.13) for the function $F(p)$ and the following equation for $\hat{\eta}_m$

$$\frac{d}{d\eta}\left[(1-\mu^2)\frac{d\hat{\eta}_m}{d\mu}\right] - \frac{m^2}{1-\mu^2}\hat{\eta}_m - \left(\frac{2\Omega}{c} + \frac{a^2 f_0^2}{gh}\right)\hat{\eta}_m = 0 \tag{4.3}$$

Table 6. *Values of phase speed for Rossby waves in deg. long. day^{-1} computed from quasi-geostrophic theory* ($S = a^2 f_0^2/gh$)

		$S_1 = 8.5$			$S_2 = 46.3$			$S_3 = 68.6$		
Height		$m=1$	$m=2$	$m=3$	$m=1$	$m=2$	$m=3$	$m=1$	$m=2$	$m=3$
even	c_1	−68.3	−49.5	−35.0	−14.9	−13.8	−12.3	−10.2	−9.7	−8.9
odd	c_2	−49.5	−35.0	−25.2	−13.8	−12.3	−10.9	−9.7	−8.9	−8.1
even	c_2	−35.0	−25.2	−18.7	−12.3	−10.9	−9.4	−8.9	−8.1	−7.3
odd	c_3	−25.2	−18.7	−14.3	−10.9	−9.4	−8.1	−8.1	−7.3	−6.5
even	c_3	−18.7	−14.2	−11.2	−9.4	−8.1	−7.0	−7.3	−6.5	−5.8

It is seen that (4.3) has solutions of the form

$$\hat{\eta}_m = A\,P(m, n, \mu) \tag{4.4}$$

where A is a constant provided the phase speed c is equal to

$$c = -\frac{2\Omega}{n(n+1) + \dfrac{a^2 f_0^2}{gh}} \tag{4.5}$$

where gh has values as obtained in I.

It is a straightforward matter to compute values of c from (4.5). We note that the numerical values of c are somewhat arbitrary depending on the numerical value selected for f_0, the standard value of the Coriolis parameter. In order to ease the comparison between the values computed from (4.5) and those listed in Table 4 we have for each value of m, the zonal wave number, and of the equivalent depth selected a value of f_0 which gives agreement between the two values for the component (m, m). The values of c computed from (4.5) on this basis are given in Table 6. The unit is deg. long. day^{-1}.

We notice that there are no quasi-geostrophic wave speeds equivalent to those found in the first row of Table 4. These waves were characterized by a rather large ratio between divergence and vorticity as seen from Table 5. The comparison between Table 4 and Table 6 shows, furthermore, that the quasi-geostrophic wave speeds are numerically larger than those given in Table 4, indicating a somewhat faster motion from east to west in the quasi-geostrophic case.

5. Concluding remarks

The main purpose of this paper has been to extend the analysis made in I to spherical geometry. While the vertical modes are the same as in I, there are significant changes in the horizontal modes, expressed here in terms of truncated series of associated Legendre functions. In addition to a determination of the phase speed of the horizontal modes for each vertical mode we have also investigated the structure of the horizontal modes and obtained a fair comparison with results based on observations.

The present analysis gives the possible modes which may exist in the atmosphere. However, due to the simplicity of the basic state all these modes are neutral, and a more realistic basic state is necessary in order to determine which modes will be dominating the atmospheric flow. The comparison with analysis based on observations indicates that the basic modes in both the vertical and horizontal directions are present in the atmosphere.

6. Acknowledgements

The author would like to thank Professor C. Dolph for several illuminating discussions relative to problems connected with this investigation, and Mr James Pfaendtner for programming the calculations.

REFERENCES

Bradley, J. H. S. 1967. The Transient Part of the Atmospheric Planetary Waves, PhD. thesis, University of Michigan. Also available as Report 06372-5-T, Department of Meteorology and Oceanography, University of Michigan, 113 pp.

Bradley, J. H. S. & Wiin-Nielsen, A. 1968. On the transient part of the atmospheric planetary waves. *Tellus 20*, 533–544.

Burger, A. P. 1958. Scale considerations of planetary motions in the atmosphere. *Tellus 11*, 195–205.

Eliasen, E. & Machenhauer, B. 1969. On the observed large-scale atmospheric wave motion. *Tellus 21*, 149–166.

Phillips, N. A. 1963. Geostrophic Motion. *Reviews of Geophysics 1*, 123–176.

Wiin-Nielsen, A. 1970. On the motion of various vertical modes of transient, very long waves. I. *Tellus 23*, 88–98.

О ДВИЖЕНИИ РАЗЛИЧНЫХ ВЕРТИКАЛЬНЫХ МОД НЕСТАЦИОНАРНЫХ УЛЬТРАДЛИННЫХ ВОЛН. ЧАСТЬ II. СФЕРИЧЕСКИЙ СЛУЧАЙ

Решается задача о движении атмосферных волн, наложенных на основное состояние покоя с постоянным градиетом температуры. Найдено, что существует несколько вертикальных мод. Для каждой вертикальной моды существует несколько горизонтальных мод, движущихся с различными скоростями и имеющих определенный меридиональный профиль геопотенциала, функции тока и потенциала скоростей. Решение находится разложением каждого переменного для каждой вертикальной моды в конечный ряд по присоединенным полиномам Лежандра. Найдено, что волны, связанные с первой вертикальной модой ведут себя как волны в однородной жидкости со свободной поверхностью, тогда как волны, связанные со второй и третьей вертикальными модами, движутся со значительно меньшими скоростями. Все волны движутся с востока на запад. Структура волн хорошо согласуется с соответствующей структурой, полученной по атмосферным наблюдениям. Решения сравниваются с движением нестационарных ультрадлинных волн, получаемых в квазигеострофической модели.